

**Regular Paper****Fields** Molecular Biology**Title:** Klotho protects chromosomal DNA from radiation-induced damage

Shinya Nakayama<sup>1,2</sup>, Jiying Sun<sup>1</sup>, Yasunori Horikoshi<sup>1</sup>, Yoshitaka Kamimura<sup>1</sup>, Takeshi Ike<sup>2</sup>,  
Shu Fujino<sup>2</sup>, Yasuha Kinugasa<sup>1</sup>, Kensuke Sasaki<sup>2</sup>, Ayumu Nakashima<sup>2</sup>, Takao Masaki<sup>2</sup>, Satoshi  
Tashiro<sup>1,\*</sup>

**Affiliations:**

<sup>1</sup> Department of Cellular Biology, Research Institute for Radiation Biology and Medicine,  
Hiroshima University, Hiroshima, Japan.

<sup>2</sup> Department of Nephrology, Hiroshima University Hospital, Hiroshima, Japan.

\* Correspondence: Satoshi Tashiro, M.D., Ph.D., Department of Cellular Biology, Research  
Institute for Radiation Biology and Medicine, Hiroshima University, Kasumi 1-2-3, Minami-ku,  
Hiroshima 734-8553, Japan; e-mail: ktashiro@hiroshima-u.ac.jp

**Running Title** Radiation-induced DNA damage protection by Klotho

**Abstract**

Klotho is an anti-aging, single-pass transmembrane protein found mainly in the kidney. Although aging is likely to be associated with DNA damage, the involvement of Klotho in protecting cells from DNA damage is still unclear.

In this study, we examined DNA damage in human kidney cells and mouse kidney tissue after ionizing radiation (IR). The depletion and overexpression of Klotho in human kidney cells reduced and increased the cell survival rates after IR, respectively. The formation of  $\gamma$ -H2AX foci, representing DNA damage, was significantly elevated immediately after IR in cells with Klotho depletion and decreased in cells overexpressing Klotho. These results were confirmed in mouse renal tissues after IR. Quantification of DNA damage by a comet assay revealed that the Klotho knockdown significantly increased the amount of DNA damage immediately after IR, suggesting that Klotho protects chromosomal DNA from the induction of damage, rather than facilitating DNA repair. Consistent with this notion, Klotho was detected in both the nucleus and cytoplasm. In the nucleus, Klotho may serve to protect chromosomal DNA from damage, leading to its anti-aging effects.

**Key Words**

Aging, DNA damage,  $\gamma$ -H2AX, ionizing radiation, Klotho

## Introduction

*Alpha-Klotho* (hereafter referred to as “*Klotho*”) is an anti-aging gene identified through findings that mice with its genetic deficiency or mutations exhibit senescent phenotypes in a variety of organs. For instance, arterial sclerosis, calcification, skin atrophy, neurodegeneration, and other age-associated problems are observed in *Klotho* knock-out mice (*kl*<sup>-/-</sup>) (1). The anti-aging function of *Klotho* is also supported by a report showing that *Klotho* overexpression extends the mouse lifespan (2). The *Klotho* gene encodes a single-pass transmembrane protein, and three isoforms have been detected: a full-length transmembrane form (~130 kDa), a shortened soluble form (65 kDa), and a secreted form (65 kDa) found in blood and urine (3,4). *Klotho* is predominantly detected in the renal tubules of the kidney, ependymal cells in the choroid plexus, the parathyroid gland, and mature germ cells (5). Previous studies demonstrated the interaction between *Klotho* and the receptor for fibroblast growth factor 23 (FGF23), a bone metabolizing hormone involved in the regulation of phosphate metabolism (6,7). Hyperphosphatemia was observed in *Klotho* knock-out mice and in aged patients with low *Klotho* levels due to chronic kidney diseases (8). However, the detailed mechanism of the anti-aging function of *Klotho* remains unexplained.

Aging seems to be closely related with DNA damage (9). Chromosomal DNA is continuously attacked by both intrinsic and extrinsic damaging agents, such as chemicals and

ionizing radiation (IR). Among the various classes of DNA damage, the double-strand break (DSB) is a hallmark of radiation-induced DNA damage and is quite serious due to the difficulty of its repair (10). Indeed, ionizing radiation has been shown to facilitate aging (11). Many proteins are involved in the protection of cells from DNA damage (12,13), and most function in DNA damage repair, such as  $\gamma$ -H2AX, a phosphorylated form of histone H2AX.  $\gamma$ -H2AX foci formed at DNA damage sites are well-known markers of the early steps of cellular responses to DSBs and facilitate DNA repair (14,15). The involvement of Klotho in protecting cells from DNA damage, however, remains unclear.

In this study, we found that the numbers of  $\gamma$ -H2AX foci after X-ray irradiation increased by the depletion and decreased by the overexpression of Klotho in human kidney 2 (HK-2) cells. Consistently, the amount of DNA damage induced by ionizing radiation was increased by the depletion of Klotho. Moreover, the cell viability after X-ray irradiation was reduced in Klotho knockdown cells. These findings were confirmed *in vivo*, using mice with the knockdown or overexpression of Klotho. Together, these results suggest that Klotho serves to protect DNA from radiation-induced damage.

## Materials and methods

### *Cell culture, plasmids, siRNAs, and ionizing radiation*

Human renal proximal tubular epithelial (HK-2) cells (RRID: CVCL\_0302) were purchased from American Type Culture Collection (ATCC) and cultured in RPMI-1640 medium (FUJIFILM Wako Pure Chemical Corporation), containing 10% fetal bovine serum (Gibco) and 1% penicillin/streptomycin (Life Technologies Corporation). Inducible Klotho expression in human kidney epithelial 293 cells was generated using the Flp-In<sup>TM</sup>T-REx<sup>TM</sup> system, according to the manufacturer's protocol (Thermo Fisher Scientific) (RRID: CVCL\_U421). These cells were cultured in DMEM (high glucose), containing 10% tetracycline-free FBS (Gibco), 5 µg/ml blasticidin S (Gibco), and 100 µg/ml hygromycin (Invitrogen). Since even without tetracycline treatment, the level of Klotho protein produced by leaky expression was approximately three-fold higher in these Klotho-expressing 293 cells than that in HK-2 cells, the experiments in this study were performed in the absence of tetracycline. All cells were incubated at 37°C in a humidified 5% (vol/vol) CO<sub>2</sub> incubator. For knockdown experiments, we purchased siRNAs (Silencer Select Pre-designed siRNA Products s2251420 and s17915; referred to as siKL-#1 and siKL-#2 in the text, respectively), s15590 (siFGF23), s5165 (siFGR), and Negative Control #2 (siNT in the text), from Life Technologies Japan Ltd. Cell transfections were performed with

Lipofectamine RNAiMAX (Invitrogen), according to the manufacturer's instructions. Ionizing irradiation treatments were performed using an X-ray generator (CP-160, Faxitron Bioptics) at the indicated doses.

### ***Western blotting***

Cell fractionation experiments were performed with NE-PER™ Nuclear Extraction Reagents or a Subcellular Protein Fractionation Kit for Cultured Cells (Thermo Fisher Scientific). Western blot analyses were performed as described previously (6, 16, 17). Primary antibodies were rat monoclonal anti-human Klotho antibody (1:330; KM2076, TransGenic Inc.), mouse anti- $\beta$ -actin (Sigma-Aldrich), mouse anti-vinculin (BC039174, Proteintech), rabbit anti-histone H3 (Abcam), mouse anti-lamin B1 (Santa Cruz), rat anti-FGF23 (#283511, Bio-Techne), and rabbit anti-FGFR (Cell Signaling). Photography was performed with a ChemiDoc MP Imaging System (Bio-Rad) and the Image Lab software (Bio-Rad).

### ***Cell Viability***

On the day before transfection,  $0.75 \times 10^4$  cells were seeded in 60 mm dishes, and then transfected with siRNAs on the next day. Afterwards, the cells were irradiated with 3 Gy or 5 Gy of X-rays. At four days after irradiation, cells were harvested and counted by a CellDrop Automated Cell Counter (DeNovix).

### ***Immunofluorescence Staining***

Immunofluorescence staining was performed as described previously (18). Briefly, cells were fixed in 4% paraformaldehyde in PBS for 10 minutes at room temperature, and then permeabilized with 0.5% Triton X-100 in PBS for 10 minutes at room temperature. The cells were incubated for 30 minutes at 37°C with a mouse monoclonal anti-phospho-histone H2AX antibody (1:40,000; Upstate), in PBS containing 1% bovine serum albumin (BSA). The secondary antibody was Cy3-conjugated goat anti-mouse antibody (1:1,000; Invitrogen). Cells were mounted using Vectashield containing DAPI (Vector Laboratories) and observed with a BZ-X710 microscope (Keyence) or an Axio Imager Z2 microscope (Carl Zeiss) equipped with the Metafer4 software (MetaSystems).

### ***Comet Assay***

After exposure to 15 Gy of ionizing radiation, the samples were immediately cooled on ice and the neutral comet content was assessed with a Single Cell Gel Electrophoresis Assay (Trevigen). Cells were stained with SYBR GOLD and observed with a BZ-X710 microscope (Keyence), and the images were analyzed by the ImageJ software (National Institutes of Health), using the OpenComet plugin. For each condition, 406 cells were counted.

### ***Mouse kidney tissues and histology***

Eight-week-old male transgenic mice were kindly provided by Dr. Hiroko Segawa and Dr. Kenichi Miyamoto (Tokushima University Graduate School). Six-week-old male  *$\alpha$ -Klotho* KO/Jcl mice were purchased from CLEA Japan, Inc. These mice were kept in an environment with ad lib drinking water and housed in a temperature- and light-controlled room at the Laboratory Animal Center of Hiroshima University. The mice were anesthetized with a mixture of medetomidine (Kyoritsu Seiyaku), midazolam (Sand), and butorphanol (Meiji Seika Pharma). In each mouse, a skin incision was made on the right side, lateral to the spine, and the intestines were laterally retracted to expose the right kidney. During irradiation, the mouse body was protected with lead plates and adjusted so that only the right kidney was irradiated. An X-ray generator (MBR-1520R-3, Hitachi Power Solutions) was used for irradiation, and the mice were exposed to 2 Gy of X-ray irradiation. Thirty minutes afterwards, the kidneys were removed, and the tissues were observed. Immunohistochemical staining was performed according to common protocols. The primary antibodies were rabbit monoclonal anti-phospho-histone H2AX antibody (1:500; Cell Signaling Technology), and rat monoclonal anti-human Klotho antibody (1:330; KM2076, TransGenic Inc.). The ImmPRESS HRP Horse Anti-Rabbit IgG Polymer Kit (undiluted; MP-7401-15, Vector Laboratories) and ImmPRESS HRP Anti-rat IgG (mouse absorbed) Polymer Kit (MP-7444, undiluted; Vector Laboratories) were used to detect the primary antibodies. Signal intensities were quantified in 5 randomly selected fields at  $\times 200$



magnification for each sample, using ImageJ (National Institutes of Health).

### ***Statistical analysis***

Results are expressed as the mean  $\pm$  standard deviation. Statistical analyses were performed using three different software packages: Microsoft Excel for Mac (Version 16.63.1), Kaleida Graph (Version 4.5.1), and Prism 8 for OS X (Version 8.4.3). Comparisons between two groups were analyzed by the student's t-test. Values of  $P < 0.05$  were considered statistically significant.

### ***Code of ethics***

Animal experiments were conducted in agreement with National Institutes of Health guidelines on the use of laboratory animals. The institutional animal care and use committee of Hiroshima University approved all experimental protocols (Permit No. 2022-210, A19-5). All efforts were made to mitigate the animals' distress and pain.

## **Results**

### ***Klotho expression-dependent cell viability after ionizing radiation***

To investigate whether Klotho plays a role in protecting cells from DNA damage, we first examined the effects of Klotho depletion on cell viability after ionizing irradiation (IR). The depletion of endogenous Klotho using two siRNAs in HK-2 cells, derived from human renal proximal tubular epithelium, was confirmed by immunoblotting analyses using anti-Klotho

antibodies (Fig. 1A). While siKL-#1 efficiently decreased the level of the endogenous Klotho protein, siKL-#2 repressed it by less than fifty percent. Under these conditions, siKL-treated cells were irradiated with 3 or 5 Gy of X-rays, and cell viabilities were examined 4 days later. The survival rates of cells after ionizing radiation were significantly reduced by the depletion of Klotho using siKL-#1, as compared with cells transfected with siNT or siKL-#2 (Fig. 1B). The cell survival rate was lower in siKL-#2-transfected cells than in siNT-transfected cells.

To confirm the involvement of Klotho in this process, we generated human embryonic kidney cells, 293 cells, stably overexpressing GFP-fused Klotho (Fig. 1C). The level of Klotho protein was approximately three-fold higher in these Klotho-expressing 293 cells than that in HK-2 cells. We examined the effect of Klotho overexpression on the cell viability after X-ray irradiation. The survival rate of Klotho overexpressing cells was significantly higher than that of the parental cells (Fig. 1D). Taken together, these findings suggest that Klotho plays a role in protecting cells from IR.

#### ***Reduction of IR-induced DNA damage by Klotho***

To investigate whether Klotho increases cell viability after IR by protecting cells from IR-induced DNA damage, we examined the effect of Klotho depletion on  $\gamma$ -H2AX focus formation, a DNA damage marker, after IR. An immunofluorescence staining analysis was performed to detect  $\gamma$ -H2AX foci in siKL-treated cells exposed to 2 Gy of X-ray radiation. The numbers of  $\gamma$ -

H2AX foci were significantly increased after IR in HK2 cells transfected with siNT, siKL-#1 or siKL-#2 (Fig. 2A, B). Among them, siKL-#1-transfected cells showed significantly higher numbers of  $\gamma$ -H2AX foci at 0.5 and 2 hours after IR, as compared to those in siNT- or siKL-#2-transfected cells. However, there were no significant differences between these cells in terms of the numbers of  $\gamma$ -H2AX foci at 8 and 24 hours after IR. In contrast, the numbers of  $\gamma$ -H2AX foci at 0.5 hours, but not at later points, after X-ray irradiation in Klotho-overexpressing cells were lower than those in parental cells (Fig. 2C, D). Since one  $\gamma$ -H2AX focus corresponds to one DSB, the higher numbers of  $\gamma$ -H2AX foci at early time points after DNA damage induction suggest that more DNA damage occurs by the same radiation dose, rather than by slower DNA repair. Therefore, Klotho is probably involved in suppressing the induction of DNA damage by X-rays, rather than DNA repair, in HK2 cells.

To examine the amounts of DSBs induced by IR in Klotho-deficient cells, we performed a neutral comet assay, which is a method to detect DSBs. The tail moment was evaluated immediately after exposure to 15 Gy of ionizing radiation. The tail moment of cells transfected with siKL-#1 was significantly longer as compared to those of siNT- or siKL-#2-transfected cells ( $P < 0.001$ ) (Fig. 2E, F). The tail moment of cells transfected with siKL-#2 after IR was longer than that of siNT- transfected cells, but there was no significant difference. This could be due to the lower efficiency of Klotho depletion by siKL-#2 than that by siKL-#1.

These findings strongly suggest that Klotho protects chromosomal DNA from the induction of DSBs by IR.

Klotho is an imperative factor of the FGF receptor 1 (FGFR1) complex, and membrane-associated Klotho forms this complex with the co-receptor for fibroblast growth factor 23 (FGF23) and functions in phosphate metabolism (1). Therefore, we next tested the possibility that Klotho is involved in the phosphorylation of H2AX after IR through the FGF system. To address this, we analyzed the  $\gamma$ -H2AX focus formation in FGFR1- or FGF23-depleted HK-2 cells after X-ray irradiation. Unlike the case of the Klotho knockdown, an increased number of  $\gamma$ -H2AX foci was not observed (Sup. Fig. 1), implying that Klotho plays a role in DNA damage responses independently of the FGFR1 complex.

#### ***Nuclear localization of Klotho in human kidney cells***

Although Klotho has been recognized as a single-pass transmembrane protein, our findings suggested the role of Klotho in the cell nucleus to protect DNA. To examine the subcellular localization of Klotho in HK-2 cells, we performed an immunoblotting analysis of nuclear and cytoplasmic extracts using anti-Klotho antibodies. Although the signal intensity was lower as compared to that in the cytoplasm, Klotho was detected in the nuclear fractions (Fig. 3A). To examine the localization of Klotho in more detail, we performed a subcellular fractionation analysis. We separated HK-2 cells into five fractions: cytoplasmic, membrane-associated,

nuclear soluble, chromatin-bound, and cytoskeleton. As a result, Klotho was detected in all fractions. Interestingly, the level of Klotho in the chromatin-bound fraction was higher than that in the nuclear soluble fraction (Fig. 3B). These findings support the notion that Klotho functions in the human renal cell nucleus to protect DNA from IR.

***Klotho protects the kidney from ionizing radiation in vivo***

Finally, to confirm the involvement of Klotho in the protection of chromosomal DNA *in vivo*, we examined the effect of the genetic ablation of the Klotho gene on the formation of  $\gamma$ -H2AX foci after X-ray irradiation in the mouse kidney (Fig. 4A-C). We performed an immunoblotting analysis of  $\gamma$ -H2AX in the kidneys of Klotho homozygous and heterozygous knockout mice, at 0.5 hours after ionizing irradiation. As a result, the  $\gamma$ -H2AX levels were significantly higher in the Klotho homozygous knockout mice as compared to those in the heterozygous knockout and wild-type mice, suggesting that Klotho is required to reduce the radiation-induced DNA damage *in vivo* (Fig. 4D-F).

We next performed an immunohistochemistry analysis of the  $\gamma$ -H2AX levels in kidneys from irradiated wild-type and Klotho transgenic mice. The  $\gamma$ -H2AX levels after 2 Gy of irradiation were lower in the kidneys from Klotho transgenic mice than in those from wild-type mice (Sup. Fig. 2). These results are consistent with the findings obtained from the *in vitro* experiments using human cells, in that Klotho plays a role in protecting chromosomal DNA

from radiation-induced damage.

## **Discussion**

In this study, we showed that the depletion of Klotho, a transmembrane protein with an anti-aging function, led to reduced cell viability and increased DNA damage after subjecting human kidney cells to ionizing radiation *in vitro*. Interestingly, the amount of DSBs after IR was increased by the depletion of Klotho. Consistent with these findings, Klotho was detected in the chromatin-bound fraction in human kidney cells. The role of Klotho in DNA protection *in vivo* was confirmed in Klotho KO and transgenic mice. These results support our hypothesis that Klotho functions to protect DNA in human cells.

Klotho has been recognized as an “aging-suppressor” (3). A well-known function of Klotho is to reduce the blood phosphate level associated with the acceleration of aging, by increasing phosphate excretion through the formation of a co-receptor with FGF23 (7). Using a comet assay, we showed that the amount of radiation-induced DSBs detected just after IR was increased in the Klotho-depleted cells, while the kinetics of DSB repair and the reduction of the numbers of  $\gamma$ -H2AX were not affected. Many proteins are involved in the various aspects of DNA repair processes (19). For example, Dsup suppresses X-ray-induced DNA DSBs and single strand breaks (SSBs) by binding directly to DNA (20). Therefore, Klotho may have a similar function to Dsup in protecting chromosomal DNA from extrinsic DNA damaging

factors, such as IR. However, the mechanisms by which Klotho protects chromosomal DNA from IR-induced damage remain to be clarified.

Klotho- or FGF23-deficient mice exhibit early aging and are rescued, although not completely, from the aging-like phenotypes by nutrient phosphate limitation (21). Hyperphosphatemia accelerates vascular calcification and is known as an atypical risk factor for cardiovascular disease (CVD) mortality in end stage renal disease (ESRD) (22). In this study, however, no significant changes in the formation of  $\gamma$ -H2AX foci after IR were observed under the knockout conditions of FGFR or its ligand FGF23 (Sup. Fig. 1A) (6). Therefore, FGFR and FGF23 may not be involved in the DNA protection by Klotho. Still, we could not exclude the possibility that the hyperphosphatemia caused by the depletion of the Klotho-FGF system may contribute to the induction of DNA damage *in vivo*. Klotho is also known to induce the FoxO forkhead transcription factors through the inhibition of the IGF-1 signaling pathway. The FoxO forkhead transcription factors induce the expression of manganese superoxide dismutase in response to oxidative stress (23). Since IR is a type of strong oxidative stress, Klotho may protect cells from DNA damage through its various functions, in a similar manner to anti-oxidative stress factors.

Klotho exists as a co-receptor for FGF23 at the plasma membrane and is also cleaved and secreted into the blood. In this study, however, we detected the presence of Klotho in

almost all cell fractions, including the chromatin fraction. The mechanisms of Klotho traffic into the cell nucleus, for association with chromatin to protect DNA, remain to be clarified, and the important question of how Klotho, expressed only in kidney and brain, protects mice and humans from aging awaits an answer.

## References

1. Kuro-o, M., Matsumura, Y., Aizawa, H., Kawaguchi, H., Suga, T., Utsugi, T., Ohyama, Y., Kurabayashi, M., Kaname, T., and Kume, E. (1997) Mutation of the mouse *klotho* gene leads to a syndrome resembling ageing. *Nature* **390**, 45-51
2. Kurosu, H., Yamamoto, M., Clark, J. D., Pastor, J. V., Nandi, A., Gurnani, P., McGuinness, O. P., Chikuda, H., Yamaguchi, M., Kawaguchi, H., Shimomura, I., Takayama, Y., Herz, J., Kahn, C. R., Rosenblatt, K. P., and Kuro-o, M. (2005) Suppression of aging in mice by the hormone Klotho. *Science* **309**, 1829-1833
3. Kuro-o, M. (2010) Klotho. *Pflugers Arch* **459**, 333-343
4. Xu, Y., and Sun, Z. (2015) Molecular basis of Klotho: from gene to function in aging. *Endocr Rev* **36**, 174-193
5. Li, S. A., Watanabe, M., Yamada, H., Nagai, A., Kinuta, M., and Takei, K. (2004) Immunohistochemical localization of Klotho protein in brain, kidney, and reproductive



- organs of mice. *Cell Struct Funct* **29**, 91-99
6. Kurosu, H., Ogawa, Y., Miyoshi, M., Yamamoto, M., Nandi, A., Rosenblatt, K. P., Baum, M. G., Schiavi, S., Hu, M. C., Moe, O. W., and Kuro-o, M. (2006) Regulation of fibroblast growth factor-23 signaling by Klotho. *J Biol Chem* **281**, 6120-6123
  7. Kuro-o, M. (2021) Aging and FGF23-klotho system. *Vitam Horm* **115**, 317-332
  8. John, G. B., Cheng, C. Y., and Kuro-o, M. (2011) Role of Klotho in aging, phosphate metabolism, and CKD. *Am J Kidney Dis* **58**, 127-134
  9. Schumacher, B., Garinis, G. A., and Hoeijmakers, J. H. (2008) Age to survive: DNA damage and aging. *Trends Genet* **24**, 77-85
  10. Jeggo, P. A., and Löbrich, M. (2007) DNA double-strand breaks: their cellular and clinical impact? *Oncogene* **26**, 7717-7719
  11. Richardson, R. B. (2009) Ionizing radiation and aging: rejuvenating an old idea. *Aging (Albany NY)* **1**, 887-902
  12. Setlow, P. (2007) I will survive: DNA protection in bacterial spores. *Trends Microbiol* **15**, 172-180
  13. Martinez, A., and Kolter, R. (1997) Protection of DNA during oxidative stress by the nonspecific DNA-binding protein Dps. *J Bacteriol* **179**, 5188-5194
  14. Kuo, L. J., and Yang, L. X. (2008) Gamma-H2AX - a novel biomarker for DNA

- double-strand breaks. *In Vivo* **22**, 305-309
15. Klovov, D., MacPhail, S. M., Banáth, J. P., Byrne, J. P., and Olive, P. L. (2006) Phosphorylated histone H2AX in relation to cell survival in tumor cells and xenografts exposed to single and fractionated doses of X-rays. *Radiother Oncol* **80**, 223-229
  16. Doi, S., Zou, Y., Togao, O., Pastor, J. V., John, G. B., Wang, L., Shiizaki, K., Gotschall, R., Schiavi, S., Yorioka, N., Takahashi, M., Boothman, D. A., and Kuro-o, M. (2011) Klotho inhibits transforming growth factor- $\beta$ 1 (TGF- $\beta$ 1) signaling and suppresses renal fibrosis and cancer metastasis in mice. *J Biol Chem* **286**, 8655-8665
  17. Fujino, S., Sun, J., Nakayama, S., Horikoshi, Y., Kinugasa, Y., Ishida, M., Sakai, C., Ike, T., Doi, S., and Masaki, T. (2022) A Combination of Iohexol Treatment and Ionizing Radiation Exposure Enhances Kidney Injury in Contrast-Induced Nephropathy by Increasing DNA Damage. *Radiat Res* **197**, 384-395
  18. Sun, J., Shi, L., Kinomura, A., Fukuto, A., Horikoshi, Y., Oma, Y., Harata, M., Ikura, M., Ikura, T., and Kanaar, R. (2018) Distinct roles of ATM and ATR in the regulation of ARP8 phosphorylation to prevent chromosome translocations. *Elife* **7**, e32222
  19. Chatterjee, N., and Walker, G. C. (2017) Mechanisms of DNA damage, repair, and mutagenesis. *Environ Mol Mutagen* **58**, 235-263
  20. Hashimoto, T., Horikawa, D. D., Saito, Y., Kuwahara, H., Kozuka-Hata, H., Shin, I. T.,

- Minakuchi, Y., Ohishi, K., Motoyama, A., Aizu, T., Enomoto, A., Kondo, K., Tanaka, S., Hara, Y., Koshikawa, S., Sagara, H., Miura, T., Yokobori, S. I., Miyagawa, K., Suzuki, Y., Kubo, T., Oyama, M., Kohara, Y., Fujiyama, A., Arakawa, K., Katayama, T., Toyoda, A., and Kunieda, T. (2016) Extremotolerant tardigrade genome and improved radiotolerance of human cultured cells by tardigrade-unique protein. *Nat Commun* **7**, 12808
21. Kuro-o, M. (2018) Molecular Mechanisms Underlying Accelerated Aging by Defects in the FGF23-Klotho System. *Int J Nephrol* **2018**, 9679841
22. Giachelli, C. M. (2009) The emerging role of phosphate in vascular calcification. *Kidney Int* **75**, 890-897
23. Yamamoto, M., Clark, J. D., Pastor, J. V., Gurnani, P., Nandi, A., Kurosu, H., Miyoshi, M., Ogawa, Y., Castrillon, D. H., Rosenblatt, K. P., and Kuro-o, M. (2005) Regulation of oxidative stress by the anti-aging hormone Klotho. *J Biol Chem* **280**, 38029-38034

## Figure Legends

### Fig. 1 Effects of Klotho depletion or overexpression on cell viability after IR

- (A) Expression of Klotho protein in HK-2 cells, with or without Klotho knockdown. (siNT: Negative control, siKL-#1: s225120, siKL-#2: s17915).  $\beta$ -actin was used as a loading

control. Band intensities were analyzed and normalized to  $\beta$ -actin by densitometry.

(B) Viability of irradiated HK-2 cells, with or without Klotho knockdown. Data are shown as mean  $\pm$  SE of three independent experiments. \* $P < 0.05$ , \*\* $P < 0.01$  (t-test).

(C) Protein levels of Klotho in Flp-In<sup>TM</sup> T-Rex 293 cells expressing GFP-tagged Klotho.

(D) Cell viability of Flp-In<sup>TM</sup> T-Rex 293 cells expressing GFP-tagged Klotho after IR. Data are shown as mean  $\pm$  SE of three independent experiments. \* $P < 0.05$  (t-test).

**Fig. 2 Requirement of Klotho in the reduction of IR-induced DNA damage**

(A) Representative images of  $\gamma$ -H2AX foci in HK-2 cells at 0.5 hours after IR.

Immunofluorescence staining was performed using anti- $\gamma$ -H2AX antibodies. Scale bar: 10  $\mu$ m.  $\gamma$ -H2AX: red, DAPI (DNA): blue.

(B) Number of  $\gamma$ -H2AX foci in HK-2 cells at 0.5, 2.0, 8.0 and 24 hours after 1 Gy of IR.

(C) Representative images of  $\gamma$ -H2AX foci in parental and KL-GFP-expressing 293 cells at 0.5 hours. Immunofluorescence staining was performed using anti- $\gamma$ -H2AX antibodies. Scale bar: 10  $\mu$ m.  $\gamma$ -H2AX: red, DAPI (DNA): blue.

(D) Numbers of  $\gamma$ -H2AX foci in parental or KL-GFP-expressing 293 cells at 0.5, 2.0, 8.0 and 24 hours after 1 Gy of IR. Data are shown as mean  $\pm$  SE of three independent experiments. \*\* $P < 0.01$  (t-test).

(E) Representative comet assay images of HK-2 cells with or without X-ray exposure. DNA

was stained by SYBR GOLD.

- (F) The tail moments of HK-2 cells detected by a neutral comet assay after 15 Gy of IR. After IR, the cells were immediately placed on ice, and then 406 cells were analyzed in each experiment. Data are shown as mean  $\pm$  SE of three independent experiments.  $**P < 0.01$ ,  $***P < 0.001$  (t-test).

### **Fig. 3 Intracellular localization of Klotho**

- (A) HK-2 cells were fractionated using a NE-PER<sup>TM</sup> Nuclear and cytoplasmic extraction kit. Histone H3 was used as a nuclear indicator and GAPDH as a cytoplasmic indicator. Band intensities were analyzed and normalized to  $\beta$ -actin by densitometry.
- (B) HK-2 cells were fractionated using a subcellular protein fractionation kit. Vinculin was the indicator of the cytoplasmic and membrane fractions. Histone H3 was the indicator of the chromatin fraction. Lamin B1 was used as an indicator of the nuclear cytoskeleton.

### **Fig. 4 $\gamma$ -H2AX in Klotho knockout and transgenic mice after IR**

- (A) Klotho immunohistochemical staining of kidney tissues of wild-type (+/+), hetero- (*kl/+*) or homo- (*kl/kl*) Klotho knockout mice irradiated by 2 Gy of X-rays. Scale bar: 100  $\mu$ m.
- (B) Klotho expression in wild-type (+/+), hetero- (*kl/+*), and homo- (*kl/kl*) Klotho knockout mice was quantified by an immunoblotting analysis using anti-Klotho antibodies. The extracts of kidney tissue from the three types of mice were analyzed (n= 3).

- (C) Quantification of the Klotho expression shown in (B). The amounts of Klotho were normalized to GAPDH.  $**P < 0.01$  (t-test), (n= 3).
- (D)  $\gamma$ -H2AX immunohistochemical staining of  $\gamma$ -H2AX kidney tissues of wild-type (+/+), hetero- (*kl/+*) or homo- (*kl/kl*) Klotho knockout mice after 2 Gy irradiation. Scale bar: 50  $\mu$ m.
- (E) Immunoblotting analysis of  $\gamma$ -H2AX using kidney tissue extracts from wild-type (+/+), hetero- (*kl/+*) or homo- (*kl/kl*) Klotho knockout mice after 2 Gy irradiation, using anti- $\gamma$ -H2AX antibodies. Histone H3 was used as a loading control (n= 3).
- (F) Quantification of the  $\gamma$ -H2AX shown in (E). The amounts of Klotho were normalized to histone H3. The three types of mice were analyzed (n= 3).

Fig.1

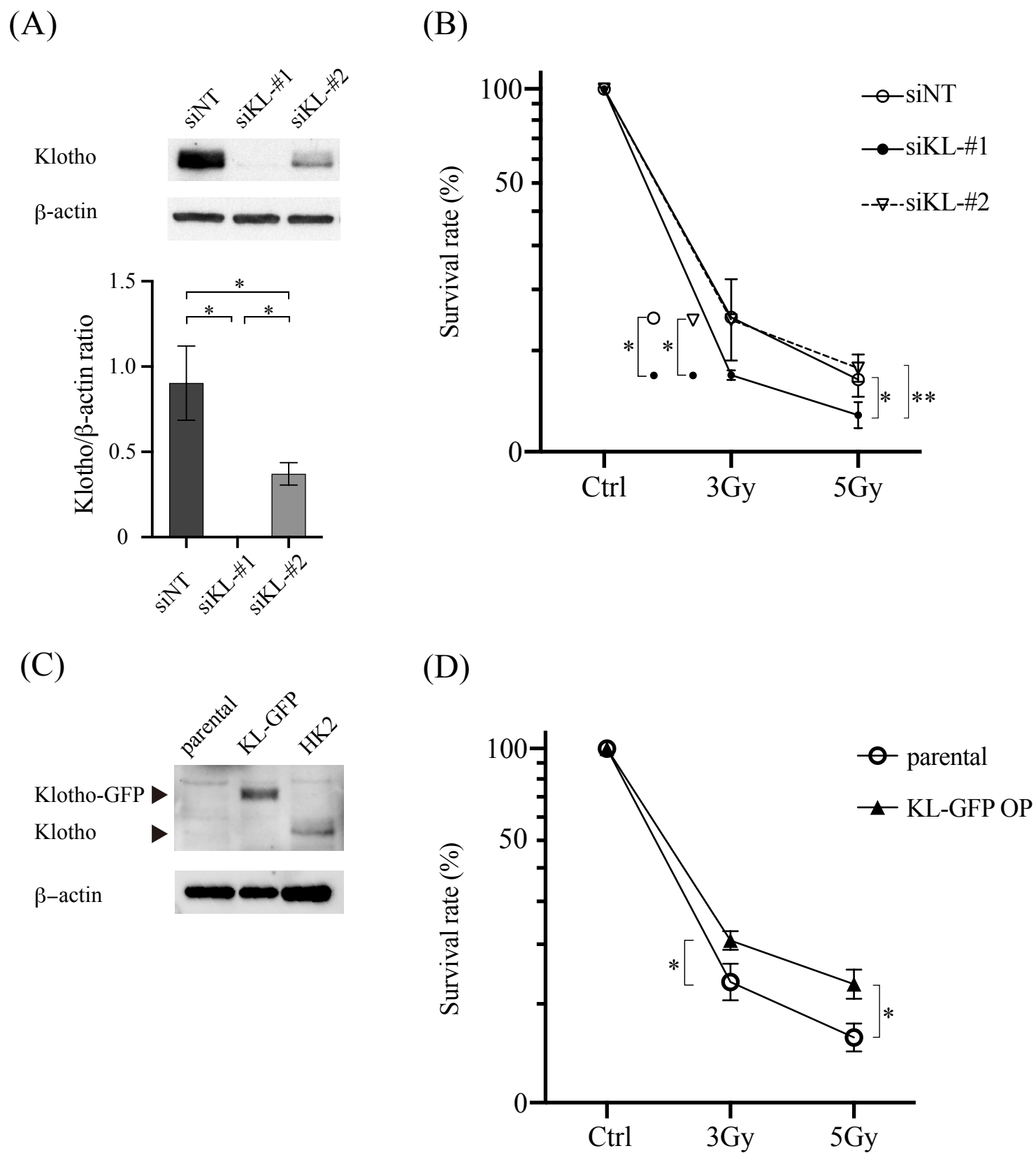


Fig.2

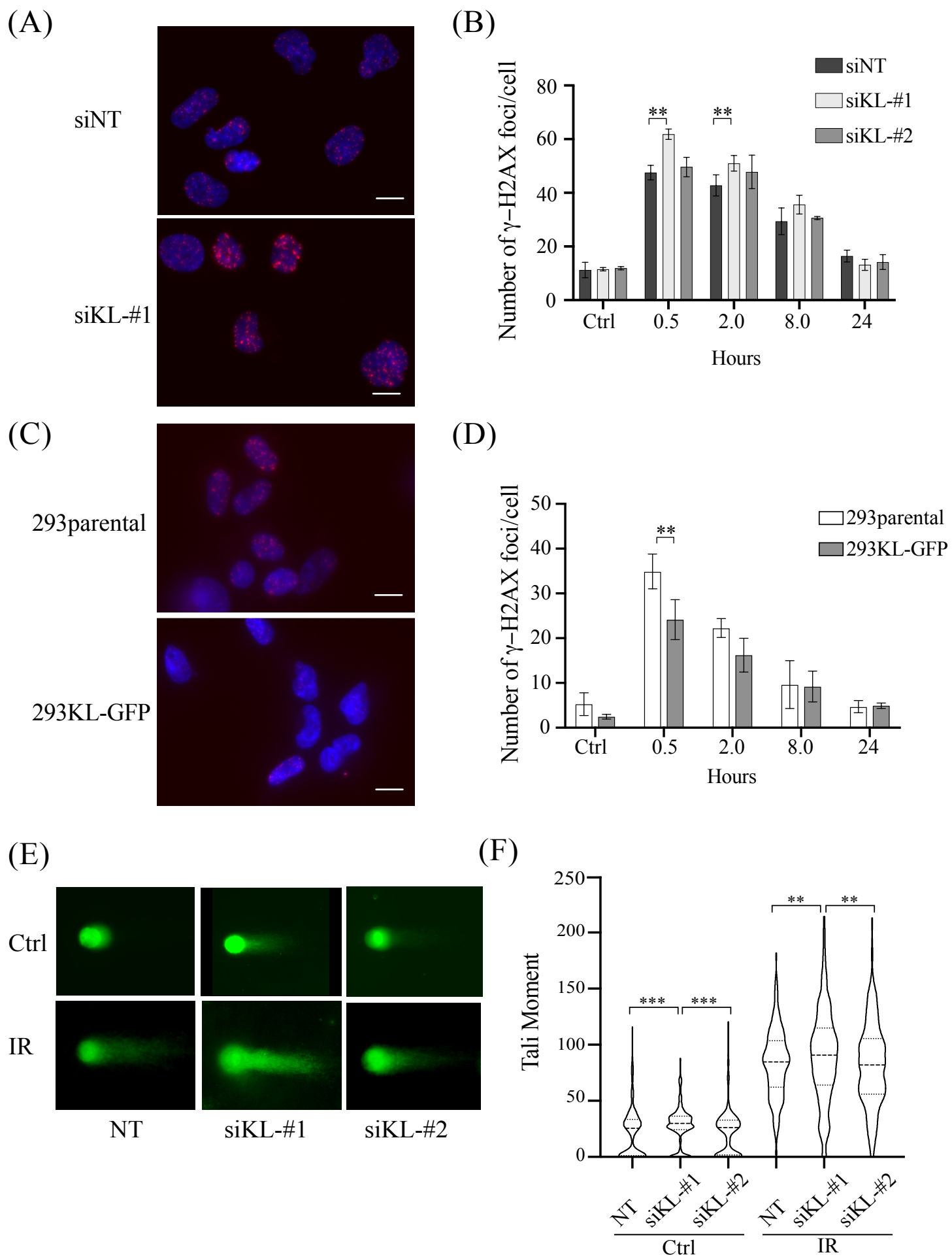
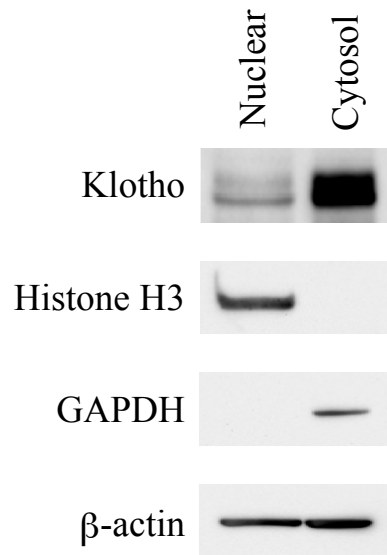




Fig.3

(A)



(B)

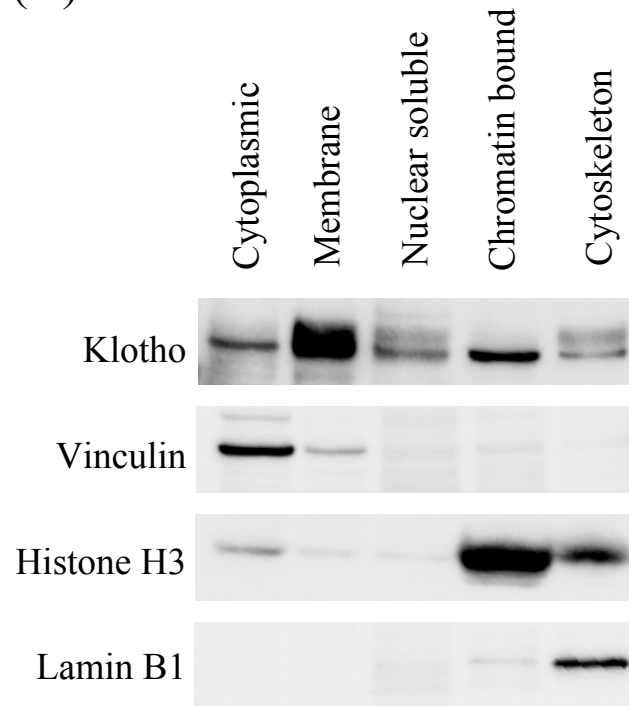
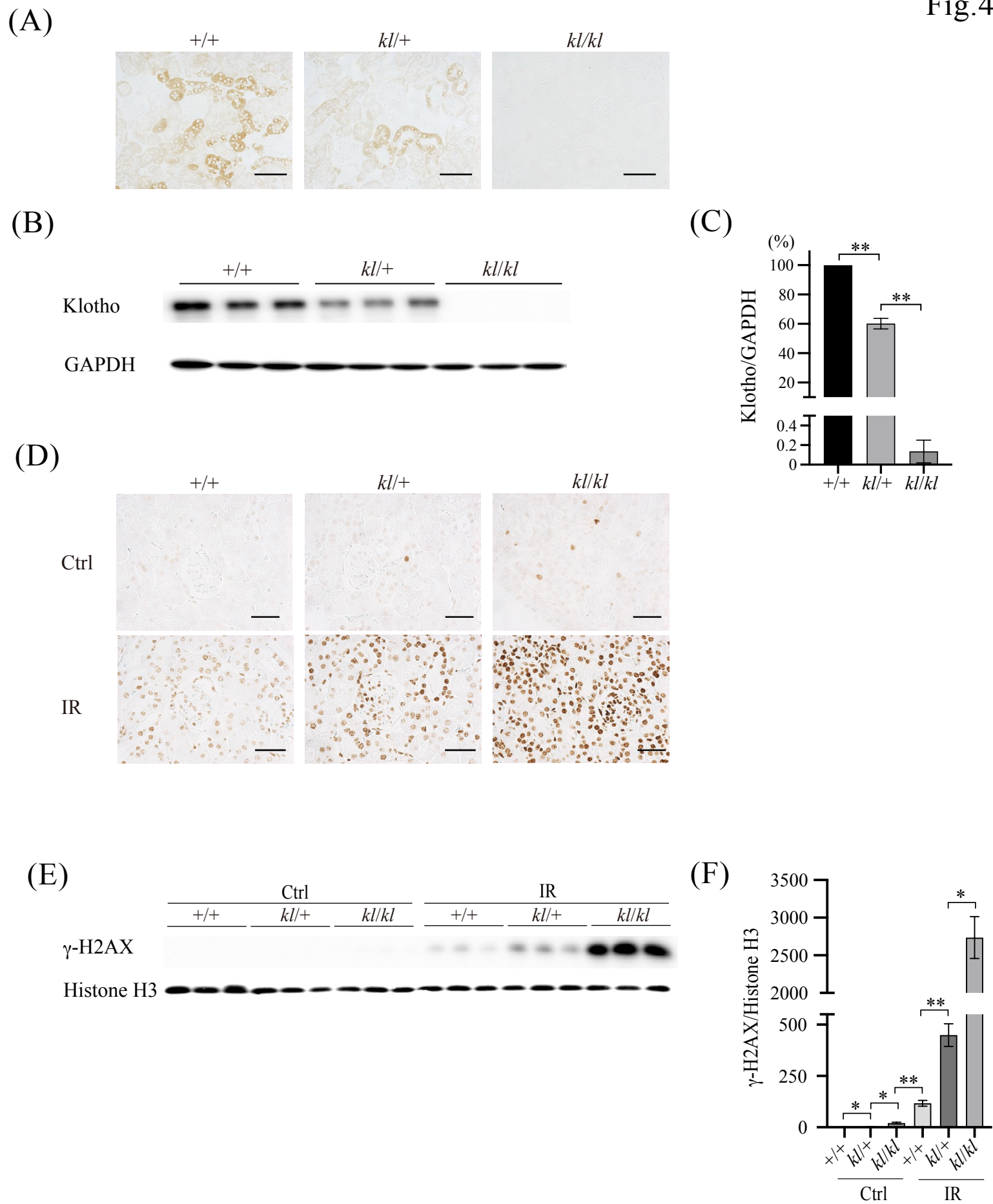


Fig.4



## Supplementary Data

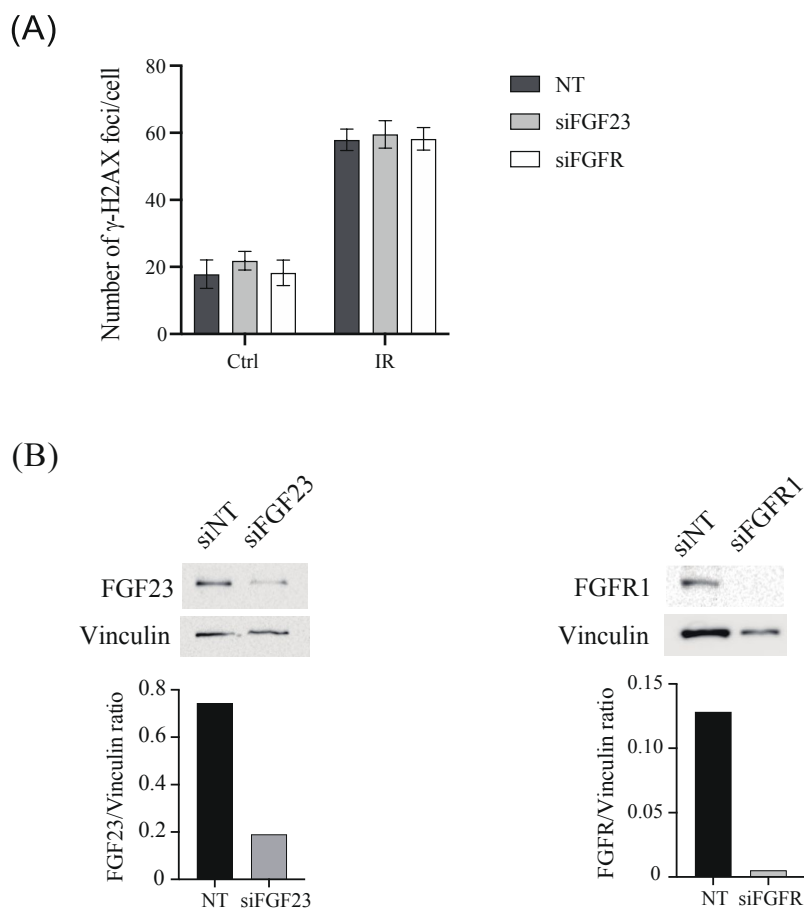
## Supplemental Fig.1

Effects of FGF23 or FGFR knockdown on irradiation-induced  $\gamma$ -H2AX foci formation

(A) Numbers of  $\gamma$ -H2AX foci in HK-2 cells expressing siFGF23 or siFGFR at 0.5 hours after 1 Gy of IR. Data are shown as mean  $\pm$  SE of three independent experiments.

(B) Expression of FGF23 or FGFR protein in HK-2 cells with or without FGF23 or FGFR knockdown. (siNT: Negative control, siFGF23: s15590, siFGFR: s5165). Band intensities were analyzed and normalized to vinculin by densitometry.

## Supplement Fig.1



**Supplemental Fig.2**

- (A)  $\gamma$ -H2AX immunohistochemical staining of kidney tissue of wild-type (WT) or Klotho transgenic (Kl-Tg) mice after 2 Gy irradiation. Scale bar: 100  $\mu$ m.
- (B) Quantification of the  $\gamma$ -H2AX shown in (A).  $*P < 0.05$  (t-test).
- (C) Klotho immunohistochemical staining of kidney tissue of wild-type (WT) or Klotho transgenic (Kl-Tg) mice after 2 Gy irradiation. Scale bar: 100  $\mu$ m.
- (D) Quantification of the Klotho shown in (C).  $*P < 0.05$  (t-test).

## Supplement Fig.2

